URSI GASS 2021, Rome, Italy, 28 August - 4 September 2021

Modeling Windblown Forest Clutter For SAR simulations

Husson Xavier[(1)(2)], Lepetit Thomas[(1)], Trouve Nicolas[(1)] and Boust Fabrice[(1)]
(1) ONERA, The French Aerospace Lab, DEMR - Electromagnetism and Radar
(2) xavier.husson@onera.fr

Abstract

In this paper we present a complete radar modeling pipeline for windblown forest clutter. Because the forest is a set of trees, as a first approach, we model an isolated tree. For validation purposes our pipeline is adapted to SAR simulations. For this model the emphasis was put on 3 characteristics : tree animation due to wind, usage of frequencies higher than the S-band and possibility to be representative of the environment. To evaluate the backscattered field an asymptotic EM method was used combining geometrical and physical optics.

1 Introduction

SAR imaging allows the imaging of the Earth's surface with nearly no disadvantage due to meteorological conditions. It is used in many domains such as measuring melting ice speed, forecasting earthquakes... Nevertheless, it is a method that needs a lot of means (airborne systems, antennas, operators). Another limitation is that it can be difficult to acquire specific areas with these airborne systems. Therefore simulations are used to evaluate the robustness and the precision of processing algorithm or to increase databases size.
In order to be able to realize a representative simulation, one should be able to model each components of the scene, either targets (cars, tanks, boats...) or clutters (sea, forest). One of the characteristics of forest clutter is the Doppler shift induced by the wind. This aspect compromises a lot of processing algorithms. This is the focus of this paper.

Since the sixties and the emergence of FOPEN [1] (Foliage Penetration) many vegetation models were developed[2] but there seems to be no models adapted to both animation and SAR imaging. For frequencies higher than the S-band (C, X, Ku...), the canopy cannot be considered transparent anymore. In that regard it is needed to model trees as a whole.
Different approaches exist in the literature to design trees as presented in the survey from Zhang and Pang [3]. In order to generate typical trees fitted for animation and with a fine level of precision, we decided to use a 3D surfacic mesh representation [4].
To render tree animation and evaluate the backscattered field, a hybrid asymptotic approach is chosen based on the geometrical and physical optics approximations.

First we present the mean used to generate 3D surfacic tree mesh. Then we present our asymptotic approach. A focus is then made on tree animation time dependency. All these aspects allow us to compose our modeling pipeline for simulation purposes. Lastly we present simulation results in the form of SAR images.

2 3D surfacic mesh modeling

To model our trees and to be able to generate typical trees (in opposition to a specific tree) we decided to use a tree modeling software : SpeedTree [4]. This software allows us to generate a 3D surfacic mesh representation for each modeled tree. Figure 1 shows an example of a tree generated by SpeedTree. SpeedTree major advantages for our model are as follow.
Because SpeedTree modeling is based on a hierarchical construction concept, it allows a procedural approach and therefore a large diversity of trees modeling possibilities (broad leaf, conifer, palm tree...). Besides, the use of randomization process allows to easily generate multiple trees of a same type.
In addition, SpeedTree includes a wind-based animation model.

3 High frequency backscattering

3.1 Asymptotic method

In our approach we uncovered 2 levels of complexity due to the usage of a 3D mesh-based representation : one on a global scale and one on a local scale.
For the global parameter we looked at 2 aspects of the representation : spatial and time. Spatially, the dimensions of the tree, as a whole, are largely greater than the wavelength (3cm for the X-band for example). For the time-based aspect the problem is as follow, the more our mesh is animated the more meshes have to be generated. This can be considered as another meshed object being added. In that regard, one of the constraint of our model is the use of a fast numerical method.
In addition, in our 3D surfacic mesh, the smaller elements are either leaves or branches on the rim. Their characteristic dimensions are greater than the wavelength for the X-band

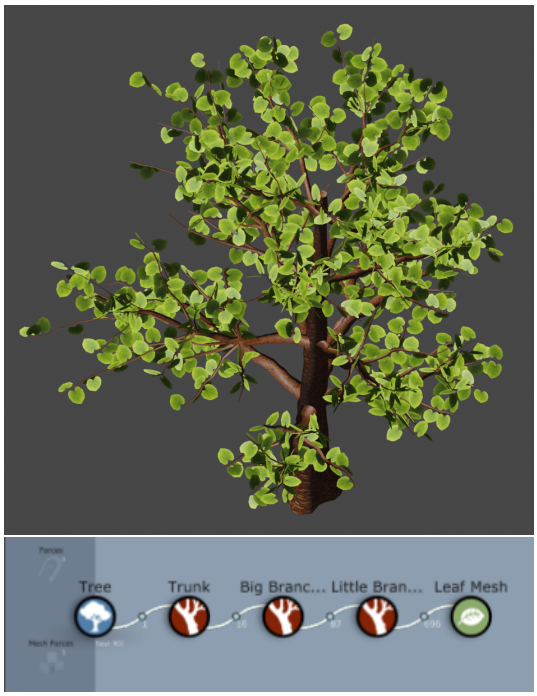

Figure 1. Example of a broadleaf tree modeled with SpeedTree[4]. The chart under the 3D model represents the hierarchical levels of conception.

or higher frequencies band. Therefore it is possible to use an asymptotic method.
For all these reasons, we chose a numerical EM asymptotic method able to render the animation composed of 2 steps : a visibility step based on geometrical optics and a scattering calculation based on physical optics.

3.2 Backscattering

From the well-known Maxwell equations, one can reformulate the scattering problem by using the Stratton-Chu equations. Under the physical optics approximations these equations can be further simplified to obtain for the electric field E Equation (1) (similar results can be obtain for the magnetic field H)

$$\overrightarrow{E_s}(\overrightarrow{r}) = \frac{e^{-jkR_0}}{4\pi R_0}\overrightarrow{\alpha_E}\left(\underline{\underline{R}}, \overrightarrow{E_0}\right)\iint_S e^{-j(\vec{k}_0^i - \vec{k}_0^s).\vec{r}'}dr' \quad (1)$$

with $\overrightarrow{E_s}$ the scattered electric field, $\overrightarrow{E_0}$ the incident wave polarization, $\underline{\underline{R}}$ the Fresnel reflectivity coefficients matrix, $\vec{k}_0^i$ and $\vec{k}_0^s$ the incident and scattered wave vectors, $\vec{\alpha}_E$ a function of 2 variables.
This equation can be split into 3 factors. The first factor can be associated to a spherical wave. The second factor $\vec{\alpha}_E$ is material and polarization dependent. The third factor, the double integral, is geometry dependent.

For the second factor, the polarization parameter can be determine using acquisition parameters. The reflectivity matrix is linked to the Fresnel's coefficients. These coefficients can be determine using the vegetation permittivity. In our model we used an empirical permittivity model based on Debye-Cole dual-dispersion model[5] from the literature[6]

$$\varepsilon_v = \varepsilon_{dv} + v_{fw}\varepsilon_{fw} + v_{bw}\varepsilon_{bw} \quad (2)$$

with ε_{dv} the real part of the relative permittivity of bulk vegetation, v_{bw} and v_{fw} are the bound and free water volume fraction, ε_{bw}, and ε_{fw} correspond to bound and free water permittivities[6].

To evaluate the double integral, a method was proposed in the case of a closed polygonal surface by Gordon [7]. This approach was later reformulated with a more general expression by McInturff and Simon [8]. In our study, we are working with a surfacic 3D meshed object, thus the use of such a method is suitable.

4 Time dependency

The two main time constants of SAR acquisitions (or simulations) are the pulsed duration *pD* and the Pulse Repetition Interval (*PRI* or its frequency equivalent *PRF*). In case of SAR acquisition, objects are usually considered static in regards to the pulse duration.
In our model, to render the Doppler Shift induced by the wind, our trees should be animated at the same frequency as the *PRF*. For trees, experimental campaigns measured natural frequencies for trees movements between 0.1 and 10 Hertz [9] [10] (depending on the tree characteristics and the measured part position). While comparing tree natural frequencies and the *PRF*, one cannot consider trees static between pulses but it should also be noted that while it should have an impact on the Doppler shift, the visibility between consecutive pulses should not change drastically.
In that regard, when no analytic formulation exists to calculate the positions of the mesh nodes at the *PRF*, we decided to interpolate these position in-between the animation frames. As mentioned in section 2, we used the SpeedTree animation model[4]. Because both the positions and the speed of the mesh nodes are known, a second order interpolation was implemented.

5 Modeling pipeline

We present here the main steps of our modeling pipeline. Figure 2 provides an illustration.
First a 3D surfacic tree mesh is generated with the SpeedTree software [4]. Second the tree mesh is animated to render wind-related movements using the software Blender [11].
Because we decided to use a hybrid electromagnetic asymptotic approach the 2 next steps focus on geometrical and physical optics. Third is indeed the use of ray-tracing to extract the visible contributors of our mesh. The POV-Ray [12] software was used because we had prior knowledge

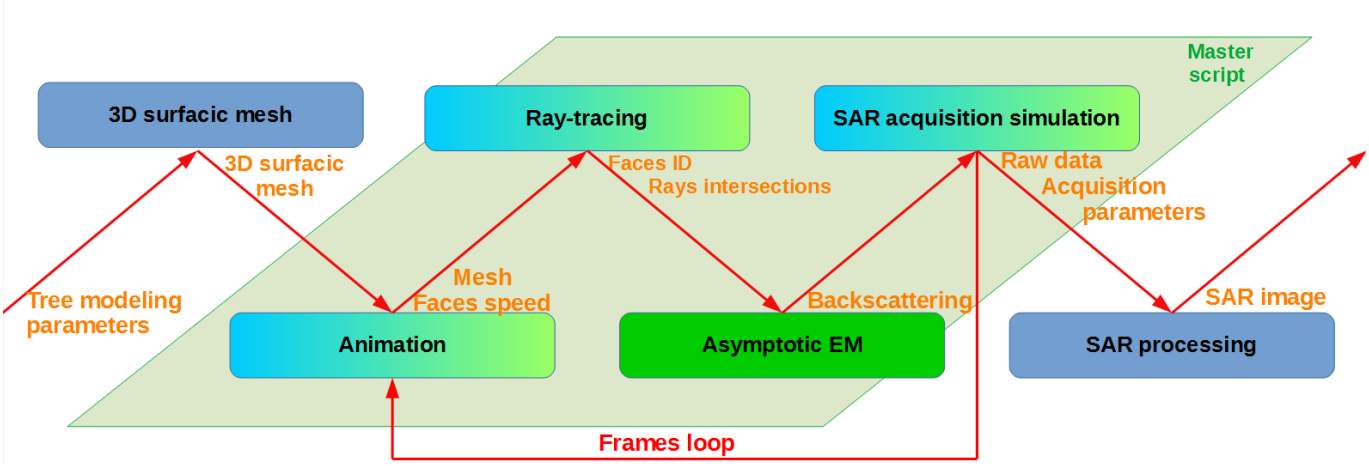

Figure 2. Modeling pipeline. Green modules correspond to the pipeline core, while blue modules provide the input 3D mesh and the output SAR image.

of this software. Fourth consists in evaluating the scattered field based on the physical optics approximations.
Because we want a model adapted to SAR simulations, two more steps are added. Fifth a SAR airborne system is simulated in order to emulate an acquisition to generate raw SAR data. Sixth the raw data are compressed in azimuth and distance to form a SAR image.

6 Results

Figure 3 shows a static SAR image obtained with our pipeline. Here the term static means that our tree is not under wind constraint and therefore is motionless. Indeed to simulate a SAR acquisition our fictional carrier is still animated throughout the simulation.

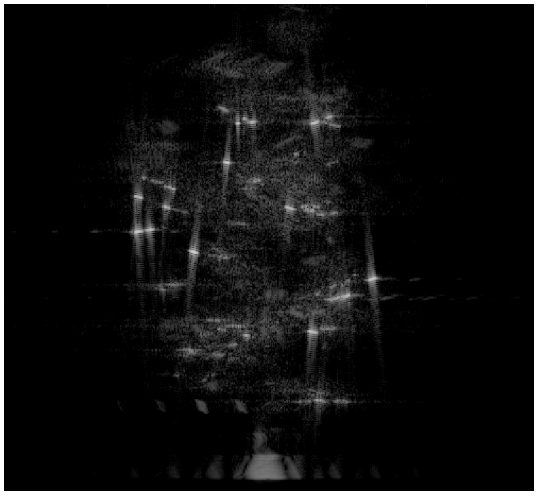

Figure 3. Simulated SAR image of a static tree $f_0 = 9.6$ GHz, $B = 3$ GHz, image resolution : 5 cm by 5 cm

Figure 4 and Figure 5 are SAR images obtained with the same tree as in Figure 3 but for two different wind strengths. In both case the same acquisition parameters were used as in the static case.

As expected in both cases, the trunk base is visibly similar to the static image for both wind strengths. Indeed it can be verified on the animation that the trunk base does not move during the acquisition.
Another expected result is that the defocus on the images, induced by along-track and cross-track movements assimilated to the Doppler shift, is correlated to the movements amplitude and frequency and therefore the wind strength. The stronger the wind the larger the blur is.

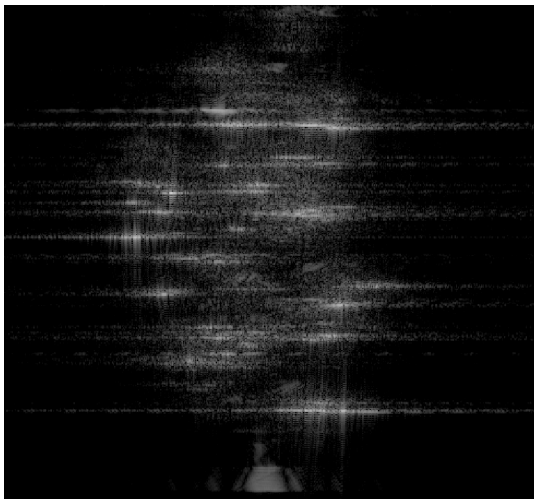

Figure 4. Simulated SAR image of a dynamic tree for a weak wind

In order to further study our model, Figure 6 shows a real SAR image including an isolated tree subject to wind. The data were acquired by the ONERA during an acquisition campaign in 2004.
An in-depth comparison cannot be made between this image and our simulation because in order to emulate this acquisition all parameters should be known (not only the carrier parameters but also the wind speed, the tree specificities...) which is not the case here. Nevertheless we can observe the azimuthal blur illustrated in our model.

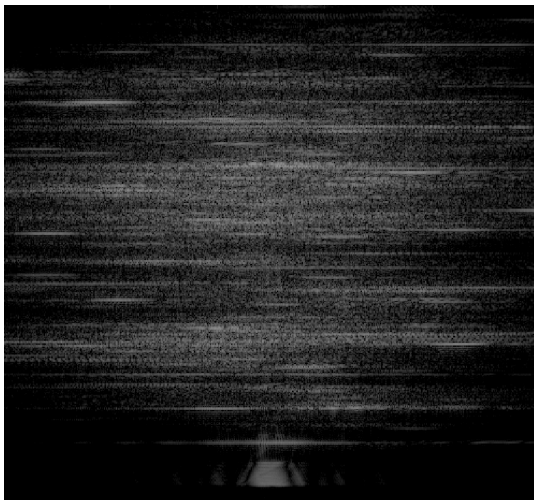

Figure 5. Simulated SAR image of a dynamic tree for a strong wind

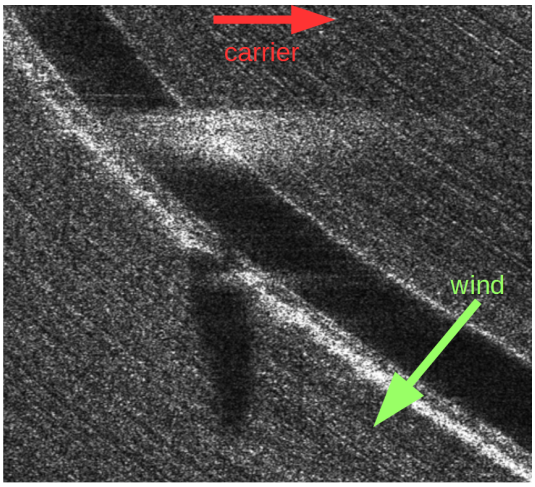

Figure 6. SAR image of an isolated tree near a road from an ONERA's acquisition campaign in X-Band. On the lower half the tree shadow is visible. On the upper half, the tree is not focused due to its movement during the acquisition

7 Conclusion

We presented here a first step towards the realization of a windblown forest clutter model, namely that of an isolated tree. This model accounts for different tree aspects : procedural tree generation, wind animation, suitable for radio frequencies higher than the S-band.
A modeling pipeline was produced in order to implement our model. This pipeline is characterize by its modularity. In addition, this model and each of its steps are evolutive (each step can be freely complexified). It allowed us to adapt it to SAR imaging for validating purposes.
Indeed a first visual comparison with real SAR images showed the capability of our model to render movement blur due to wind.
The perspectives of our model are as follows. First no multi-bounce were accounted for. It should be ensured to take them into account for our next model. Second we only represented a tree in our approach. Another focus should be on the modeling of entire forest to render a clutter sized component.

8 Acknowledgements

We would like to thanks the TSRE unit from the Departement of Electromagnetism and Radar of the ONERA and more specifically Joseph Martinot-Lagarde and Philippe Martineau for the SAR image of an isolated tree.

References

[1] D. Mark Edward, "Foliage penetration radar : detection and characterization of objects under trees", 2011.

[2] H. J. Eom, A. K. Fung, "A scatter model for vegetation up to Ku-band", Remote Sensing of Environment 15, n°3 (june 1984): 185-200.

[3] Q.-L. Zhang , M.-Y. Pang, "A survey of modeling and rendering trees", Edutainment 2008. Lecture Notes in Computer Science, vol 5093, Springer, Berlin, Heidelberg.

[4] IDV, 2016, Speedtree, http://www.speedtree.com/.

[5] F. T. Ulaby, M. A. El-Rayes, "Microwave Dielectric Spectrum of Vegetation", IEEE Transactions on Geoscienceand Remote Sensing, n°5 (1987): 541-556.

[6] ITU-R P.527-5, "Electrical characteristics of the surface of the Earth", August 2019.

[7] W. B. Gordon, "Far-Field Approximations to the Kirchhoff-Helmholtz Representations of Scattered Fields", IEEE Transactions on Antennas and Propagation (July 1975): 590-592.

[8] K. McInturff, P. S. Simon, "The Fourier Transform of Linearly Varying Functions with Polygonal Support", IEEE Transactions on Antennas and Propagation, n°39 (September 1991): 1441-1443.

[9] C.J Baker, "Measurements of the Natural Frequencies of Trees", Journal of Experimental Botany 48, n°5 (1997): 1125-32, doi: 10.1093/JXB/48.5.1125.

[10] L. Tadrist, M. Saudreau, P. Hémon, X. Amandolese, A. Marquier, T. Leclercq, and E. de Langre, "Foliage Motion under Wind, from Leaf Flutter to Branch Buffeting", Journal of The Royal Society Interface 15, n°142 (31 May 2018).

[11] Community, B.O., 2018. Blender, Stichting Blender Foundation, Amsterdam. Available at: http://www.blender.org.

[12] Persistence of Vision Pty. Ltd. (2004) Persistence of Vision Raytracer [Computer software]. Retrieved from http://www.povray.org/download/.